

## Supporting Information

### Enhancing the Efficiency and Stability of Two-Dimensional Dion-Jacobson Perovskite Solar Cells using a Fluorinated Diammonium Spacer

Di Wang<sup>a,b</sup>, Shan-Ci Chen<sup>a</sup> and Qingdong Zheng<sup>a</sup>

<sup>a</sup>State Key Laboratory of Structural Chemistry, Fujian Institute of Research on the Structure of Matter, Chinese Academy of Sciences, 155 Yangqiao West Road, Fuzhou, Fujian 350002, China

<sup>b</sup>School of Physical Science and Technology, ShanghaiTech University, 100 Haik Road, Shanghai 201210, China

#### Materials

Hydroiodic acid (HI) (57 wt.% in water, stabilized with 1.5 wt.% hypophosphorous) was purchased from Aladdin. The SnO<sub>2</sub> colloid precursor was purchased from Alfa Aesar (Tin (IV) oxide, 15% in H<sub>2</sub>O colloidal dispersion). Lead iodide (PbI<sub>2</sub>), methyl ammonium iodide (MAI), methyl ammonium chloride (MACl), bis(trifluoromethane)-sulfonimide lithium salt (Li-TFSI), and 4-*tert*-butylpyridine (TBP) were purchased from Xi'an Polymer Light Technology Crop., *N,N*-dimethylformamide (DMF), dimethylsulfoxide (DMSO), and isopropanol (IPA) were obtained from Sigma-Aldrich. 2,2',7,7'-Tetrakis[*N,N*-di(4-methoxyphenyl)amino] -9,9'-spirobifluorene (Spiro-OMeTAD) was purchased from Shenzhen Feiming Science and Technology Co., Ltd..

#### Material Synthesis

*2,3,5,6-Tetrafluoro-1,4-benzenedimethan ammonium iodide ((TFBDA)I<sub>2</sub>)*

2,3,5,6-Tetrafluoro-1,4-benzenedimethanamine (TFBDA) was synthesized using the previously

reported procedure.<sup>1</sup> HI (3 mL) was added to a solution of TFBDA (2 g, 0.01 mol) in ethanol (20 mL) under ice bath. The reaction was stirred for 12 h at room temperature. The precipitate was then washed three times with diethyl ether. The purified white powder ((TFBDA)I<sub>2</sub>) was dried in vacuum oven overnight. Physical data: <sup>1</sup>H NMR (400 MHz, D<sub>2</sub>O) δ = 4.3 (s). <sup>13</sup>C NMR (101 MHz, D<sub>2</sub>O) δ = 30.9, 113.1, 145.1 (d, J<sub>CF</sub> = 245 Hz). Elemental analysis (%): Calcd for C<sub>8</sub>H<sub>10</sub>F<sub>4</sub>I<sub>2</sub>N<sub>2</sub>: C, 20.71; H, 2.17; N, 6.04. Found: C, 20.81; H, 2.11; N, 6.09.

*1,4-Benzenedimethan ammonium iodide ((BDA)I<sub>2</sub>)*

1,4-Benzenedimethan ammonium iodide ((BDA)I<sub>2</sub>) was obtained by the reaction between pxylylenediamine (2 g) and HI (5 mL) in 20 mL of ethanol under an ice bath.<sup>2</sup> The precipitate was then washed three times with diethyl ether and recrystallized twice in ethanol. The purified white powder ((TFBDA)I<sub>2</sub>) was dried in vacuum oven overnight. Physical data: <sup>1</sup>H NMR (400 MHz, D<sub>2</sub>O) δ = 4.1 (s, 4H), 7.40 (s, 4H). <sup>13</sup>C NMR (101 MHz, D<sub>2</sub>O) δ = 42.7, 129.6, 133.4. Elemental analysis (%): Calcd for C<sub>8</sub>H<sub>14</sub>I<sub>2</sub>N<sub>2</sub>: C, 24.51; H, 3.60; N, 7.15. Found: C, 24.68; H, 3.51; N, 7.16.

*(TFBDA)PbI<sub>4</sub> crystals*

Solid PbI<sub>2</sub> (5 g, 0.01 mol) and (TFBDA)I<sub>2</sub> (5.01 g, 0.01 mol) were mixed in DMF (5 mL) in a round bottom flask. The produced yellow precipitates were dissolved by heating to 400 K to a clear solution. Slowly cooling the solution resulted in the formation of luminous yellow crystals ((TFBDA)PbI<sub>4</sub>).

*(BDA)PbI<sub>4</sub>•DMF crystals*

PbI<sub>2</sub> (5 g, 0.01 mol) and (BDA)I<sub>2</sub> (4.25 g, 0.01 mol) were mixed in DMF (5 mL) in a round bottom flask. The produced yellow precipitates were dissolved by heating to 400 K to a clear solution. Slowly cooling the solution resulted in the formation of yellow crystals ((TFBDA)PbI<sub>4</sub>).

**Preparation of 2D and 3D Perovskite Precursor Solutions**

(TFBDA)PbI<sub>4</sub> (n = 1). The (TFBDA)I<sub>2</sub> (0.7 mmol, 0.3247 g) and PbI<sub>2</sub> (0.7 mmol, 0.3227 g) were added into a mixed solvent of DMF and DMSO (900 μL+ 100 μL). The solution was stirred overnight at 50°C inside the glove box.

(TFBDA)(MA)Pb<sub>2</sub>I<sub>7</sub> (n = 2). The (TFBDA)I<sub>2</sub> (0.35 mmol, 0.1623 g), MAI (0.35 mmol, 0.0556 g), MACl (0.15 mmol, 0.01 g), and PbI<sub>2</sub> (0.7 mmol, 0.3227 g) were added into a mixed solvent of

DMF and DMSO (900  $\mu$ L+ 100  $\mu$ L). MACl was also introduced as an additive to further enhance the device performance according to the reported procedure.<sup>3</sup> The solution was stirred overnight at 50°C inside the glove box.

(TFBDA)(MA)<sub>2</sub>Pb<sub>3</sub>I<sub>10</sub> (n = 3). The (TFBDA)I<sub>2</sub> (0.23 mmol, 0.1082 g), MAI (0.47 mmol, 0.0742 g), MACl (0.2 mmol, 0.013 g), and PbI<sub>2</sub> (0.7 mmol, 0.3227 g) were added into a mixed solvent of DMF and DMSO (900  $\mu$ L+ 100  $\mu$ L). The solution was stirred overnight at 50°C inside the glove box.

(TFBDA)(MA)<sub>4</sub>Pb<sub>5</sub>I<sub>16</sub> (n = 5). The (TFBDA)I<sub>2</sub> (0.14 mmol, 0.0649 g), MAI (0.56 mmol, 0.0890 g), MACl (0.25 mmol, 0.016 g), and PbI<sub>2</sub> (0.7 mmol, 0.3227 g) were added into a mixed solvent of DMF and DMSO (900  $\mu$ L+ 100  $\mu$ L). The solution was stirred overnight at 50°C inside the glove box.

(TFBDA)(MA)<sub>9</sub>Pb<sub>10</sub>I<sub>31</sub> (n = 10). The (TFBDA)I<sub>2</sub> (0.07 mmol, 0.0324 g), MAI (0.63 mmol, 0.1001 g), MACl (0.3 mmol, 0.02 g), and PbI<sub>2</sub> (0.7 mmol, 0.3227 g) were added into a mixed solvent of DMF and DMSO (900  $\mu$ L+ 100  $\mu$ L). The solution was stirred overnight at 50°C inside the glove box.

(BDA)(MA)<sub>9</sub>Pb<sub>10</sub>I<sub>31</sub> (n = 10). The (BDA)I<sub>2</sub> (0.07 mmol, 0.0274 g), MAI (0.63 mmol, 0.1001 g), MACl (0.3 mmol, 0.02 g), and PbI<sub>2</sub> (0.7 mmol, 0.3227 g) were added into a mixed solvent of DMF and DMSO (900  $\mu$ L+ 100  $\mu$ L). The solution was stirred overnight at 50°C inside the glove box.

MAPbI<sub>3</sub> (3D). The MAI (1 mmol, 0.159 g) and PbI<sub>2</sub> (1 mmol, 0.461 g) were added into a mixed solvent of DMF and DMSO (900  $\mu$ L+ 100  $\mu$ L). The solution was stirred overnight at 50°C inside the glove box.

### **Device Fabrication**

The ITO substrates were cleaned by using detergent, distilled water, acetone, and isopropanol sequentially, then dried in an oven at a temperature of 130 °C. The ITO substrates were further treated with an ultraviolet ozone treatment for 15 min before depositing electron transport layers. Then, the substrate was coated with a thin layer of SnO<sub>2</sub> nanoparticle film (3%, diluted by water) at 3000 rpm for 30 s, and then annealed at 120 °C for 10 min and at 150 °C for 20 min. The substrate was removed from the hot plate (150 °C) directly to an inert gas filled glovebox where

the perovskite film was deposited. For fabrication of the perovskite films, the perovskite precursor (100  $\mu\text{L}$ ) was dropped onto the substrate, followed by a spin-coated process at 4000 rpm for 30 s. Twenty seconds before the ending of the spin process, 100  $\mu\text{L}$  of IPA were added dropwise onto the substrate. The films were annealed at 100  $^{\circ}\text{C}$  for 15 min. Next, the Spiro-OMeTAD precursor was spin-coated at 4000 rpm for 30 s, and it contains 72.3 mg of Spiro-OMeTAD, 17.5  $\mu\text{L}$  of Li-TFSI stock solution (520 mg of Li-TFSI in 1 mL of acetonitrile), 28.8  $\mu\text{L}$  of TBP. Finally, an 80 nm thick gold electrode was thermally evaporated on the film under a vacuum of  $\sim 10^{-4}$  Pa.

### Materials Characterization

$^1\text{H}$  NMR and  $^{13}\text{C}$  NMR spectra for the diammonium salt were recorded on a Nuclear Magnetic Resonance Spectrometer (AVANCE III).

### Crystal Structure Determination and Crystal Powder Characterization

The single crystal diffraction experiments were performed using a Bruker APEX-II diffractometer. The collected data were processed by the APX<sub>3</sub> software. The crystal structures of (TFBDA)PbI<sub>4</sub> and (BDA)PbI<sub>4</sub>•DMF were solved by direction method and subsequently refined by full-matrix least-squares on  $F^2$  using *SHELXLTL* software package. After considering the geometry, hydrogen atoms were added to the organic frame. The above-mentioned structure solution and refinement were conducted using the *Olex2* software. X-ray diffraction (XRD) patterns for the (TFBDA)PbI<sub>4</sub> and (BDA)PbI<sub>4</sub>•DMF crystal powder were performed on a Rigaku MiniFlex diffractometer at room temperature. The deposition numbers in the Cambridge Crystallographic Data Centre (CCDC) for crystal structures of (TFBDA)PbI<sub>4</sub> and (BDA)PbI<sub>4</sub>•DMF are 2063260 and 2063222, respectively.

To further confirm DMF in the analyzed (BDA)PbI<sub>4</sub>•DMF crystal, the IR (Fig. S8a) and  $^1\text{H}$  NMR (Fig. S8b) spectra was obtained. The IR spectrum displays one distinct band that originates from the stretching vibrations of the C=O (1647  $\text{cm}^{-1}$ ). Also, the IR spectrum show the bands that originate from the stretching vibrations of the C-N (1223 and 864  $\text{cm}^{-1}$ ) and N-C=O (699  $\text{cm}^{-1}$ ), indicating the presence of DMF in the (BDA)PbI<sub>4</sub>•DMF crystal. Furthermore, the  $^1\text{H}$  NMR spectra also indicate the existence of DMF. ( $^1\text{H}$  NMR (400 MHz, DMSO)  $\delta$  = 7.96 (s, 1H), 2.89 (s, 3H), 2.73 (s, 3H)).

### **Device Characterization**

All  $J-V$ ,  $I-V$  curves and steady-state power output of the devices were recorded using a Keithley 2400 Source Meter under simulated AM 1.5G illumination ( $100 \text{ mW cm}^{-2}$ ) with an Oriel Sol3A simulator (Newport), and the light intensity had been accurately calibrated with a National Renewable Energy Laboratory (NREL)-certified silicon reference cell. The external quantum efficiency (EQE) was measured using an EQE measurement system (Newport). FT-IR spectrum was collected using VERTEX70 spectrometer (Bruker).

### **Perovskite Film Characterization**

The absorption spectra were obtained by using a UV-Vis spectrophotometer (Perkin-Elmer, Lambda 365). By using a UV/V/NIR Fluorescence Spectrometer (Edinburgh Instruments, FLS980), the PL spectra were obtained for 2D perovskite films with an excitation wavelength of 400 nm and the TRPL spectra were measured by Laser excitation at 375 nm. X-ray diffraction (XRD) patterns for perovskite films were performed on a Rigaku MiniFlex diffractometer at room temperature. The images of scanning electron microscopy were obtained by on the Field Emission Scanning Electron Microscope (SU-8010). The root-mean-square (RMS) roughness of perovskite film was investigated by Scanning Probe Microscope (Bruker, Dimension Icon). Ultraviolet photoelectron spectra (UPS) measurements for perovskite films were carried out by using X-ray Photoelectron Spectroscopy (Thermo Fisher, ESCALAB 250Xi). All samples for the GIWAXS measurement were prepared on the  $\text{SnO}_2$ -coated Si substrates. The 2D GIWAXS patterns were acquired using a XEUSS SAXS/WAXS system at the National Center for Nanoscience and Technology (NCNST, Beijing). The wavelength of the X-ray beam is  $1.54 \text{ \AA}$ , and the incident angle was set as  $0.18^\circ$ . Scattered X-rays were detected by using a Dectris Pilatus 300 K photon counting detector.

### **Device Stability Test**

For the storage stability test, the unencapsulated 15 devices were tested every several days and stored in the ambient (40-70% RH, at room temperature). Thermal aging test of the unencapsulated devices was conducted in ambient air (40-70% RH) at  $80 \text{ }^\circ\text{C}$ .

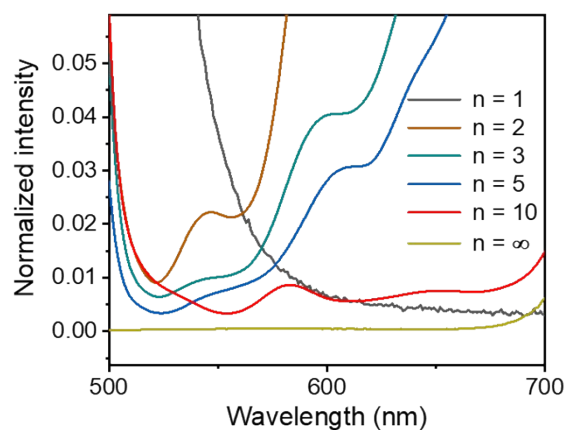


**Figure S1** Enlarged PL spectra for  $(\text{TFBDA})\text{MA}_{n-1}\text{Pb}_n\text{I}_{3n+1}$  films with different  $n$  values.

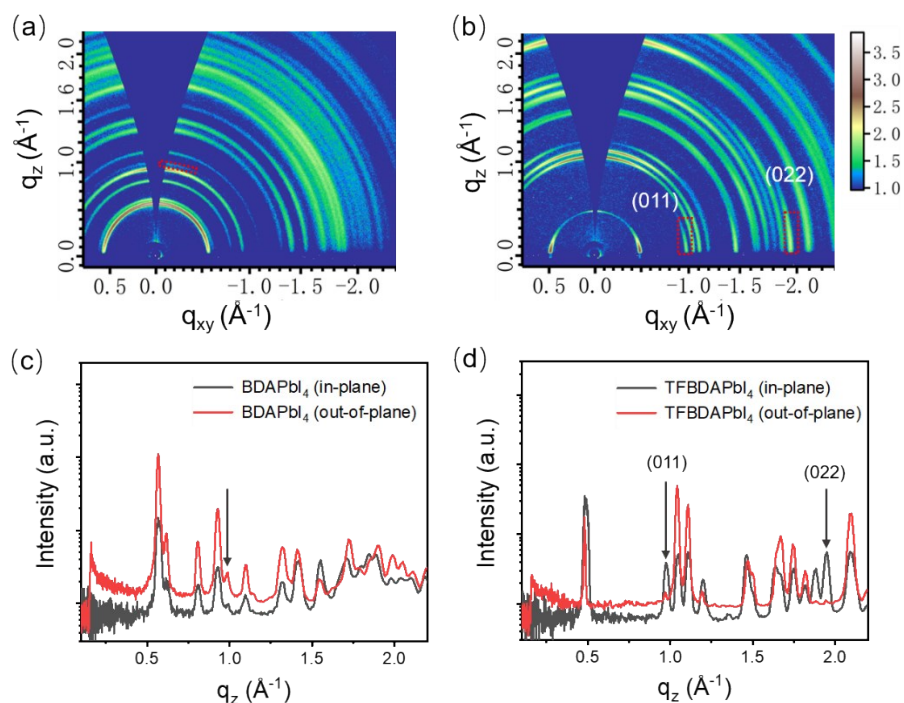


**Figure S2** 2D GIWAXS profiles of (a) 2D  $(\text{BDA})\text{PbI}_4$  film and (b)  $(\text{TFBDA})\text{PbI}_4$  films. 1D GIWAXS line profiles extracted from 2D GIWAXS profiles of (c) 2D  $(\text{BDA})\text{PbI}_4$  film and (d)  $(\text{TFBDA})\text{PbI}_4$  films (out-of-plane and in-plane direction, incident angle of  $0.14^\circ$ ).

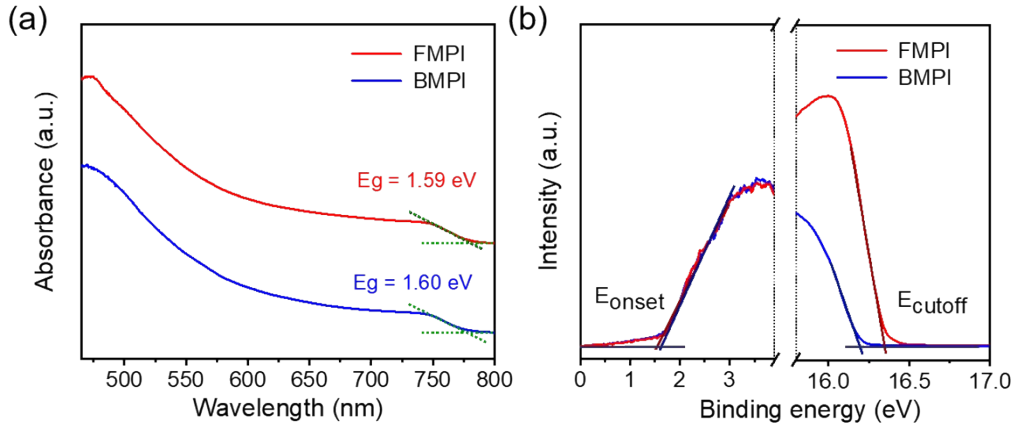


**Figure S3** (a) Comparison of absorption spectra for the perovskite films. (b) UPS measurements for the perovskite films.

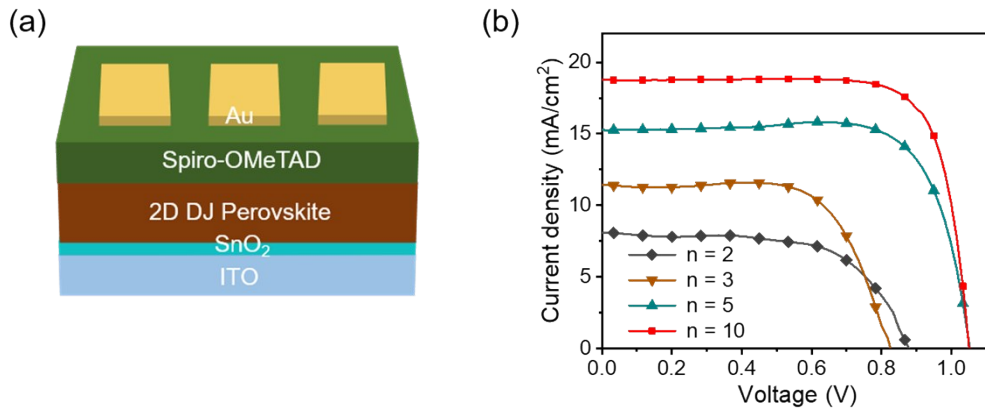


**Figure S4** (a) Device configuration of the 2D DJ PVSC. (b)  $J-V$  curves for PVSCs based on (TFBDA)MA<sub>n-1</sub>Pb<sub>n</sub>I<sub>3n+1</sub>.

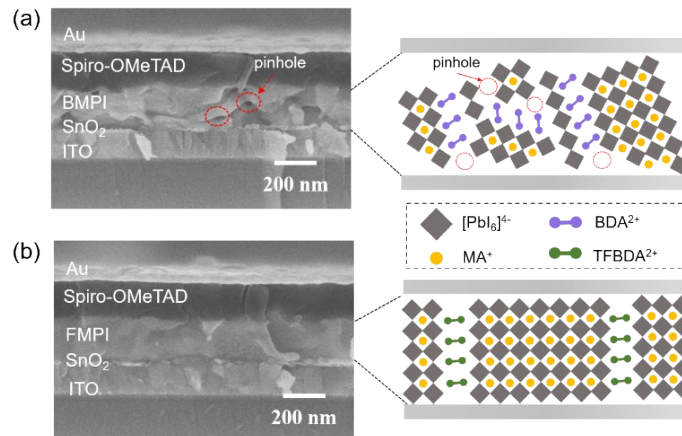


**Figure S5** Cross-section SEM images and schematic diagrams of proposed 2D slices distribution for (a) the BMPI-based device and (b) the FMPI-based device.

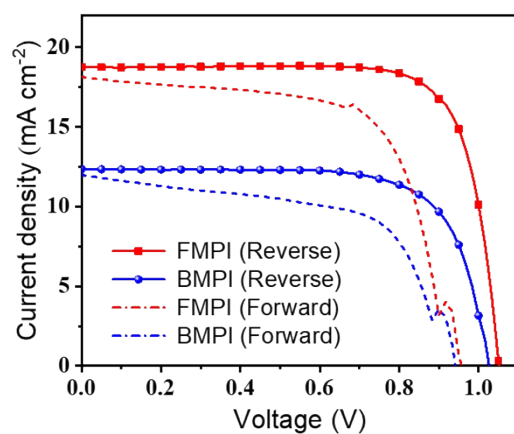


**Figure S6**  $J$ - $V$  curves for PVSCs based on BMPI and FMPI at forward and reverse scans.

**Table S1** Photovoltaic parameters of the best-performing solar cell devices

Perovskite	scan direction	$V_{oc}$	$J_{sc}$	FF	PCE	HI <sup>a</sup>
		(V)	( $\text{mA cm}^{-2}$ )	(%)	(%)	
FMPI	Reverse scan	1.05	18.76	77.31	15.24	0.26
	Forward scan	0.96	18.26	64.68	11.31	
BMPI	Reverse scan	1.03	12.39	72.14	9.16	0.26
	Forward scan	0.94	12.02	73.22	6.78	

<sup>a</sup>The hysteresis index (HI) is calculated by the formula of  $(\text{PCE}_{\text{reverse}} - \text{PCE}_{\text{forward}}) / \text{PCE}_{\text{reverse}}$ .

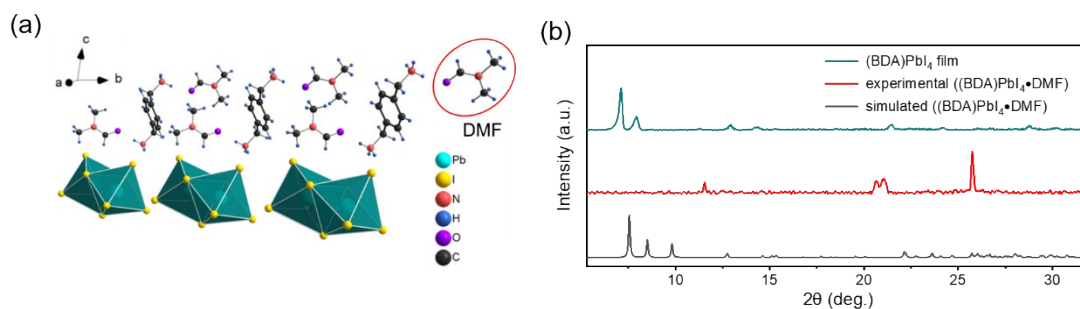


**Figure S7** (a) Single crystal structure of  $(\text{BDA})\text{PbI}_4 \cdot \text{DMF}$ . (b) Comparison of the XRD patterns for the as-made single crystal powder, the calculated patterns based on the solved single crystal structures, and the  $(\text{BDA})\text{PbI}_4$  film.



**Table S2** Crystallographic data

compound	(BDA)PbI <sub>4</sub> •DMF	(TFBDA)PbI <sub>4</sub>
Formula sum	C <sub>28</sub> H <sub>56</sub> I <sub>10</sub> N <sub>8</sub> O <sub>4</sub> Pb <sub>3</sub>	C <sub>8</sub> H <sub>10</sub> F <sub>4</sub> I <sub>4</sub> N <sub>2</sub> Pb
Formula weight	2459.37 g mol <sup>-1</sup>	924.97 g mol <sup>-1</sup>
Crystal system	triclinic	monoclinic
Space group	P-1	P2 <sub>1</sub> /c
Unit cell dimensions	a=11.1291 Å b=11.7689 Å c=13.0217 Å α=68.354° β=70.907° γ=74.918°	a=13.0472 Å b=8.5023 Å c=8.4976 Å α=90° β=97.989° γ=90°
Volume	1479.04 Å <sup>3</sup>	933.5 Å <sup>3</sup>
Z	1	2
Calculated density	2.7610 g cm <sup>-3</sup>	3.2905 g cm <sup>-3</sup>
Reflections collected	60023	5063
Independent reflections	6805 [R <sub>int</sub> = 0.0656, R <sub>sigma</sub> = 0.0330]	1371 [R <sub>int</sub> = 0.0822, R <sub>sigma</sub> = 0.0522]
F (000)	1088	804
Index ranges	-14 ≤ h ≤ 14, -15 ≤ k ≤ 15, -16 ≤ l ≤ 16	-15 ≤ h ≤ 15, -7 ≤ k ≤ 10, -10 ≤ l ≤ 10
Largest diff. peak and hole	2.162 and -2.637 eÅ <sup>-3</sup>	1.207 and -1.335 eÅ <sup>-3</sup>
Data/restrains/parameters	6805/0/248	1371/0/94
Final R indexes [I>=2σ(I)]	R <sub>1</sub> = 0.0268, wR <sub>2</sub> = 0.0583	R <sub>1</sub> = 0.0458, wR <sub>2</sub> = 0.1080
Final R indexes [all data]	R <sub>1</sub> = 0.0324, wR <sub>2</sub> = 0.0612	R <sub>1</sub> = 0.0476, wR <sub>2</sub> = 0.1104

$$R_1 = \frac{\sum||F_o| - |F_c||}{\sum|F_o|}, wR_2 = \left\{ \frac{\sum[w(|F_o|^2 - |F_c|^2)^2]}{\sum[w(|F_o|^4)]} \right\}^{1/2}, \text{ and } w = 1/(\sigma^2(I) + 0.0004I^2)$$

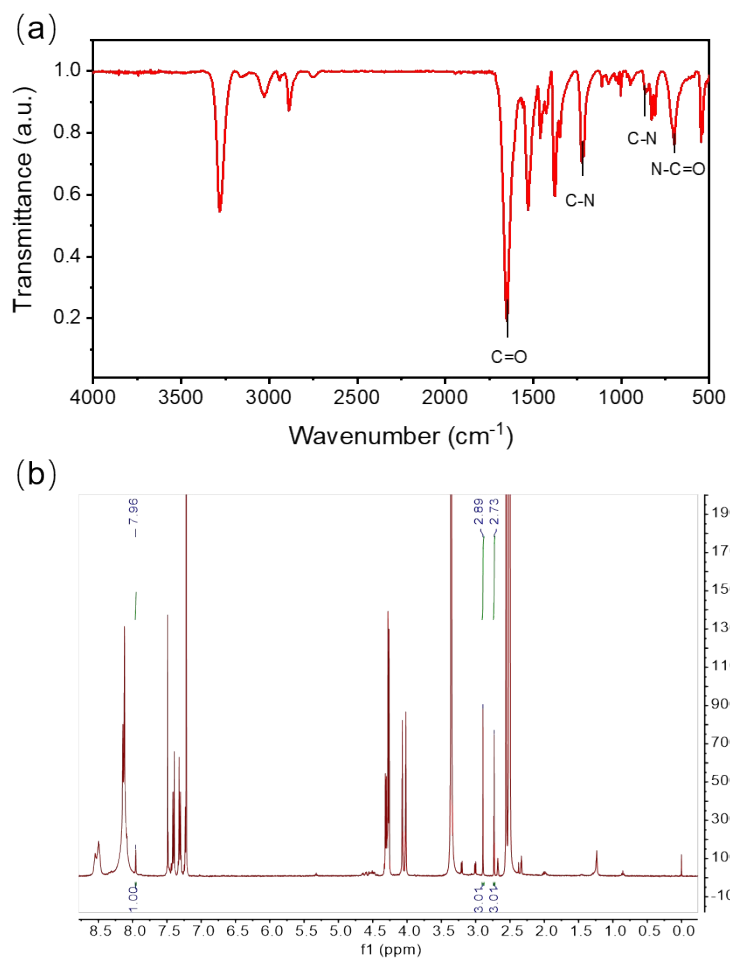


**Figure S8** (a) The FT-IR and (b) <sup>1</sup>H NMR spectra for (BDA)PbI<sub>4</sub>•DMF crystal.

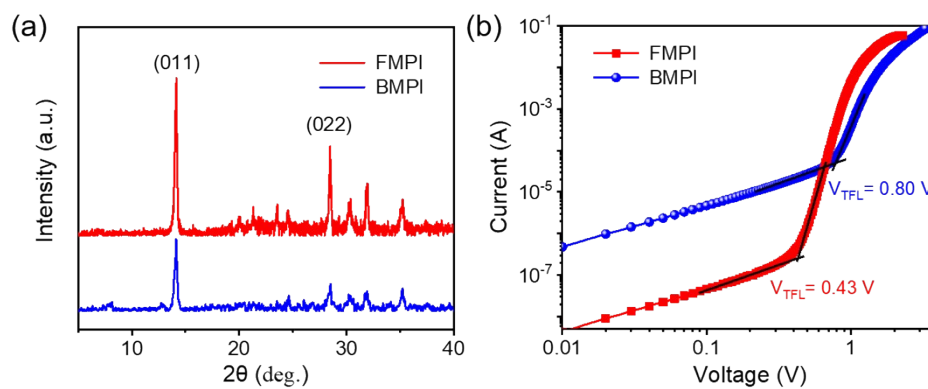


**Figure S9** (a) XRD patterns for the perovskite films. (b) *J-V* curves of electron-only devices under dark.

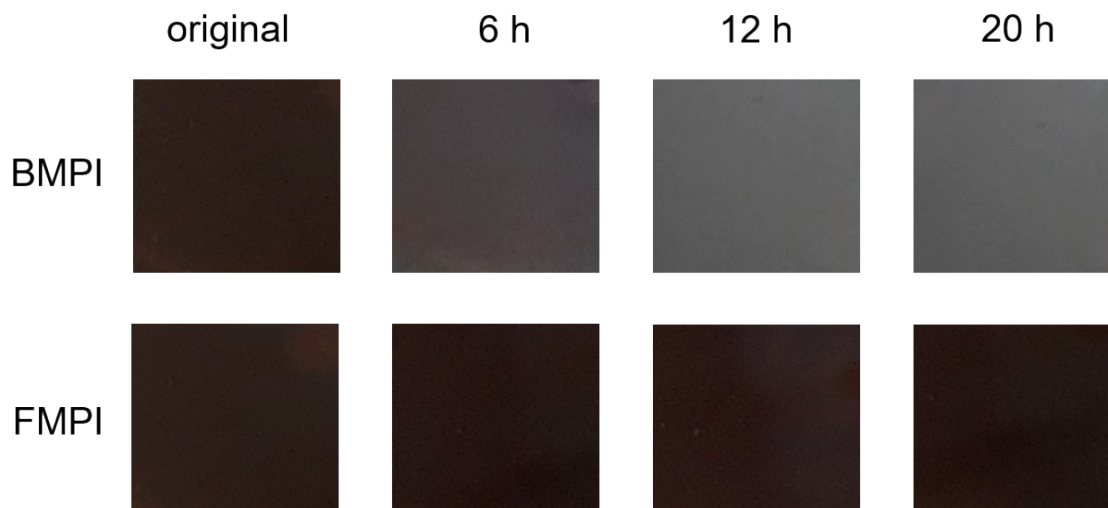


**Figure S10** Photos of perovskite films for stability test (unencapsulated BMPI and FMPI films stored in air with  $80 \pm 5\%$  RH).

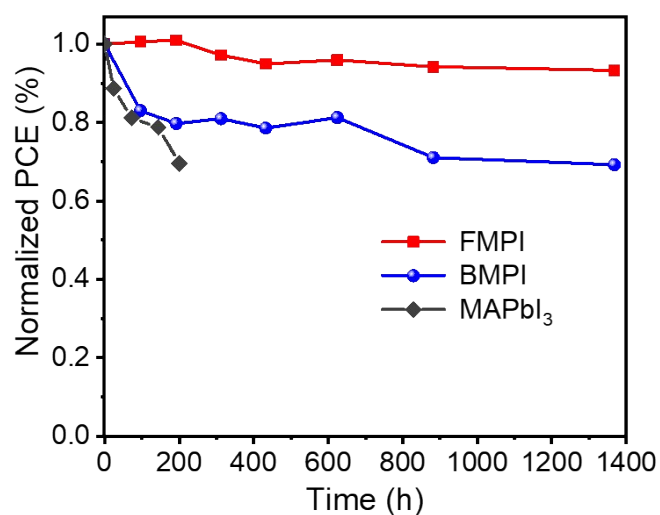


**Figure S11** Stability of 2D and 3D PVSCs.

## References

1. H. Okamoto, T. Kozai, Z. Okabayashi, T. Shinmyozu, H. Ota, K. Amimoto and K. Satake, *J. Phys. Org. Chem.*, 2017, **30**, e3726.
2. B. E. Cohen, Y. Li, Q. Meng and L. Etgar, *Nano Lett.*, 2019, **19**, 2588-2597.
3. H. T. Lai, B. Kan, T. T. Liu, N. Zheng, Z. Q. Xie, T. Zhou, X. J. Wan, X. D. Zhang, Y. S. Liu and Y. S. Chen, *J. Am. Chem. Soc.*, 2018, **140**, 11639-11646.